# Conversion of levoglucosan to glucose using an Choar tor acidic heterogeneous Amberlyst 16 catalyst

Abdilla-Santes, R. M.; Rasrendra, C. B.; Winkelman, J. G. M.; Heeres, H. J.

*Published in:*
Chemical Engineering Research & Design

*DOI:*
10.1016/j.cherd.2019.09.016



*Publication date:*
2019

Contents lists available at ScienceDirect

Chemical Engineering Research and Design

journal homepage: www.elsevier.com/locate/cherd

# Conversion of levoglucosan to glucose using an acidic heterogeneous Amberlyst 16 catalyst: Kinetics and packed bed measurements

R.M. Abdilla-Santes[a,b], C.B. Rasrendra[c], J.G.M. Winkelman[a], H.J. Heeres[a,*]

[a] Green Chemical Reaction Engineering, ENTEG, University of Groningen, Nijenborgh 4, 9747 AG Groningen, The Netherlands
[b] Department of Chemical Engineering, University of Brawijaya, MT. Haryono 167, Malang 65145, Indonesia
[c] Department of Chemical Engineering, Institut Teknologi Bandung, Ganesha 10, Bandung 40132, Indonesia

ARTICLE INFO

*Article history:*
Received 10 May 2019
Received in revised form 7 September 2019
Accepted 11 September 2019
Available online 20 September 2019

*Keywords:*
Levoglucosan
Pyrolysis
Glucose
Amberlyst 16
Kinetic model

ABSTRACT

Levoglucosan (1,6-anhydro-$\beta$-D-glucopyranose) is an anhydrosugar found in significant amounts in pyrolysis liquids obtained from lignocellulosic biomass. Levoglucosan (LG) is an attractive source for glucose (GLC), which can be used as a feedstock for biofuels (e.g. bioethanol) and biobased chemicals. Here, we report a kinetic study on the conversion of LG to GLC in water using Amberlyst 16 as the solid acid catalyst at a wide range of conditions in a batch set-up. The effects of the reaction temperature (352–388 K), initial LG intake (100–1000 mol $m^{-3}$), catalyst loading (1–5 wt%), and stirring rate (250–1000 rpm) were determined. The highest GLC yield was 98.5 mol% (388 K, 5 wt% Amberlyst 16, $C_{LG,0}$ = 500 mol $m^{-3}$ at 500 rpm stirring rate and t = 60 min). The experimental data were modelled and relevant kinetic parameters were determined using a first order approach including diffusion limitations of LG inside the Amberlyst particles. Good agreement between experiments and kinetic model was obtained. The activation energy was found to be $132.3 \pm 10.1$ kJ $mol^{-1}$. Experiments in a continuous packed bed set-up for up to 30 h show that catalyst stability is good. In addition, the steady state LG conversion (73 mol%) and the GLC selectivity were in line with the kinetic model obtained in the batch reactor.



## 1. Introduction

Lignocellulosic biomass is an abundant, sustainableand carbon-neutral renewable resource for the generation of biofuels and valuable biobased chemicals. Extensive research activities are currently commenced globally to identify techno-economically viable routes (Corma et al., 2007; Ragauskas et al., 2006; van Putten et al., 2013). Pyrolysis is an attractive method among other approaches for the conversion of lignocellulosic biomass to a liquid energy carrier, referred to as bio-oil or pyrolysis liquid. Typical liquid yields are up to 75–85 wt% of the initial biomass feed (Fast pyrolysis, 2016; Lian et al., 2010; Bennett et al., 2009) and the composition depends on the type of feedstock (biomass) and the pyrolysis conditions (Bykova et al., 2012).

Pyrolysis liquids are complex mixtures of low molecular weight acids, alcohols, furanics, aldehydes, ketones, sugar derivatives and phenolics as well as higher molecular weight sugar oligomers and lignin fragments (Oasmaa et al., 2010; Wang et al., 2013; Zacher et al., 2014). However, upon the addition of water, phase separation of the pyrolysis liquid is observed leading to a water phase enriched in polar low molecular weight molecules including the sugars derivatives (sugar fraction) and a lignin rich phase (pyrolytic lignin fraction) (Oasmaa et al., 2010; Ardiyanti et al., 2012; Elliott et al., 2009; Scholze and Meier, 2001). Both fractions can be further refined by solvent extraction protocols, among others giving a sugar fractions with high amounts of sugar derivatives. (Bennett et al., 2009; Oasmaa et al., 2010; Venderbosch et al., 2010; Rover et al., 2014; Abou-Yousef and Steele, 2013). The composition of the sugar fraction has been determined in

* Corresponding author.
E-mail address: h.j.heeres@rug.nl (H.J. Heeres).
https://doi.org/10.1016/j.cherd.2019.09.016

**Nomenclature**

| | |
|---|---|
| $A_t$ | Heat transfer area ($m^2$) |
| $C_{GLC}$ | Aqueous phase concentration of GLC (mol $m^{-3}$) |
| $C_{GLC,0}$ | Initial aqueous phase concentration of GLC (mol $m^{-3}$) |
| $C_{LG}$ | Aqueous phase concentration of LG (mol $m^{-3}$) |
| $C_{LG,0}$ | Initial aqueous phase concentration of LG (mol $m^{-3}$) |
| $C_p$ | Heat capacity of reaction mixture (J $g^{-1}$ $K^{-1}$) |
| $D_{eff}$ | Effective diffusivity of LG in the catalyst particle, $m^2$ $s^{-1}$ |
| $D_{LG}$ | Aqueous diffusivity of LG, $m^2$ $s^{-1}$ |
| $d_p$ | Catalyst average particle diameter, m |
| $E_a$ | Activation energy of LG reaction to GLC (kJ $mol^{-1}$) |
| h | Modified heat transfer coefficient from the oven to the reaction mixture ($min^{-1}$) |
| k' | Reaction rate constant based on weight of catalyst (($m^3$ liquid) (kg catalyst)$^{-1}$ $s^{-1}$) |
| $k'_{373}$ | Reaction rate constant at the reference temperature of 373 K, (($m^3$ liquid) (kg catalyst)$^{-1}$ $s^{-1}$) |
| M | Mass of the reaction mixture (g) |
| r | Catalyst particles average radius (m) |
| R | Universal gas constant, 8.3144 J $mol^{-1}$ $K^{-1}$ |
| $R_0$ | Inital rate of reaction (mol $m^{-3}$ $min^{-1}$) |
| $R'_{LG}$ | LG reaction rate based on weight of catalyst (mol (kg catalyst)$^{-1}$ $s^{-1}$) |
| SSR | Sum of squared residuals (–) |
| t | Time (min or s) |
| $T_{bulk}$ | Bulk or aqueous phase temperature (K) |
| $T_{bulk,i}$ | Initial bulk temperature (K) |
| $T_{setpoint}$ | Temperature of heating bath, setpoint for the steady state temperature (K) |
| $T_R$ | Reference temperature (K or °C) |
| U | Overall heat transfer coefficient (W $m^{-2}$ $K^{-1}$) |
| $v_s$ | Superficial velocity (m $s^{-1}$) |
| $V_{liquid}$ | Volume of liquid in the reactor ($m^3$ liquid) |
| $V_R$ | Volume of the reactor ($m^3$) |
| $W_{cat}$ | Weight of catalyst (g) |
| $X_{LG}$ | Conversion of LG (mol%) |
| $Y_{GLC}$ | Yield of GLC (mol%) |
| $(\varepsilon/\tau)$ | Porosity-tortuosity ratio of the catalyst (–) |
| $\phi$ | Thiel modulus (–) |
| $\phi_v$ | Volumetric flow rate ($m^3$ $s^{-1}$) |
| $\eta_{cat}$ | (Internal) catalyst effectiveness factor (–) |
| $\rho_{cat}$ | Density of the catalyst (kg $m^{-3}$) |

detail, and it typically consists of LG (16 wt%), glycolaldehyde (11 wt%), acids (2.5 wt%), ketones (1.4 wt%) and phenolics (0.4 wt%) (Wang, 2017), though the exact amounts are a function of the processing conditions and composition of the biomass feed.

The sugar fraction is in potential an interesting feed for the production of value-added biobased chemicals. Levoglucosan (1,6-anhydro-$\beta$-D-glucopyranose, LG), the primary degradation product of cellulose (Bennett et al., 2009; Helle et al., 2007), has been identified as the main component in the sugar fraction of pyrolysis liquids. LG can be converted into a wide variety of chemicals, among others by an initial conversion to glucose using an acid catalysed hydrolysis reaction (Scheme 1). Glucose (GLC) is an interesting starting material for value-added furan derivatives such as 5-hydroxymethylfurfural (HMF) as well as levulinic acid and lactic acid. The latter is the precursor for polylactic acid, a biodegradable biopolymer (Bozell and Petersen, 2010).

The research described in this paper is aimed to explore the use of a solid acid catalyst for the reaction of LG to GLC and to optimize the reaction conditions to obtain high GLC yields. For proper reactor design, kinetic expressions in the form of rate equations are required, which to the best of our knowledge are not reported in the literature for solid acid catalysts. The only examples involve the use of mineral acids like HCl and sulphuric acid. A kinetic study using hydrochloric acid catalyst at relatively low temperature (298–323 K) was performed by (Vidrio (2004)) and an activation energy of 97 kJ $mol^{-1}$ was reported. (Helle et al. (2007))conducted a kinetic study using sulfuric acid as the catalyst in a temperature range between 323 and 403 K and found an activation energy of 114 kJ $mol^{-1}$ and. In both studies, the effect of the initial concentration of LG was not determined and first order kinetics were assumed. Recently, we have reported a systematic experimental and modelling study of the conversion of LG to glucose in aqueous sulfuric and acetic acid solutions with good results (Abdilla et al., 2018).

The use of mineral acids as catalysts for the reaction has severe drawbacks when considering the green principles of chemistry and technology. Recycle of such acids is energy and capital intensive and often the acids are neutralised in the work-up section to produce large amounts of inorganic salts. As such, the use of solid acid catalysts is highly desirable, allowing operation in for instance packed bed configurations without the need of recycle. We here report an experimental and modelling study of the hydrolysis of LG in aqueous solution using a heterogeneous solid catalyst in the form of Amberlyst 16. To the best of our knowledge, detailed studies on LG hydrolysis in water with a solid acid catalyst and accompanying kinetic models have not been reported in the literature. This particular solid acid was selected as it is commercially available, relatively cheap compared to other ion exchange resins and has a good thermal stability of up to 403 K. The active sites are composed of sulfonic acid groups and in combination with the porous, open structure, it has shown an excellent solid catalysts for various transformations. The effects of reaction parameters (temperature, stirring rate, LG intake and catalyst loading) on the reaction rate were investigated and the relevant kinetic parameters were determined from the experimental data. The implications of the models regarding GLC yield will be discussed and finally the stability of the catalyst was investigated in a continuous set-up for extended run-times.

## 2. Experimental section

### 2.1. *Chemicals*

LG was purchased from Carbosynth, UK. GLC (≥99.5 wt%) was obtained from Sigma-Aldrich (Steinheim, Germany). Both chemicals were used without further purification Amberlyst 16 (wet) was acquired from Dow Chemicals (Chauny, France). The catalyst was washed three times with Milli-Q water and dried overnight at 50 °C (323 K) prior to use. Milli-Q water was used for all experiments.

### 2.2. *Experimental procedures*

The batch experiments were carried out in pressure tubes (Ace pressure tube bushing type, front seal, volume ~9 ml with a length of 10.2 cm and an outer diameter of 19 mm). The tubes were loaded with 5 ml LG solution (100–1000 mol $m^{-3}$) containing the appropriate amounts of the Amberlyst 16 catalyst (1, 2 and 5 wt% loading). After filling, the tubes were subsequently submerged in a temperature-controlled heating bath (352–388 K). During reaction, the mixture was stirred at 500 rpm using a Teflon stirrer. In the tubes, the pressure is about the vapour pressure of water at the selected temperature (352–388 K). In this temperature range, the pressure difference is less than 1 bar and is not expected to have a significant effect on the reaction rates. As such, pressure effects of kinetic constants were not considered. At various reaction

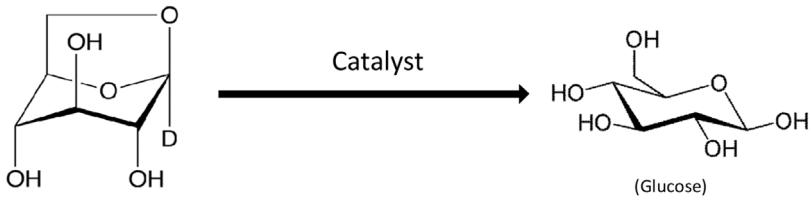


**Scheme 1 – Levoglucosan (LG) hydrolysis to glucose (GLC).**

times, a tube was taken and quickly immersed in cold water to stop the reaction. Subsequently, an aliquot of the reaction mixture was taken, diluted with Milli-Q water and analyzed by high performance liquid chromatography (HPLC).

The continuous experiments were performed in a packed-bed reactor. The setup was equipped with a pre-heater to heat the feed liquid and an air pressured pump to feed the solution to the reactor and a back pressure valve to set the pressure, see Figure S1 in the Supplementary information for details. The reactor (length of 14.3 cm and an internal diameter of 6 mm) was filled with 1.33 g of Amberlyst 16. The pre-heater has approximately the same dimensions as the reactor. The experiments were carried out at a set-point of 393 K with a feed consisting of 100 mol $m^{-3}$ of LG loading at a liquid flowrate of 2.2 ml $min^{-1}$ and the outlet pressure was set at 5 bar. At different runtimes, samples were taken from the reactor outlet, diluted with Milli-Q water and subjected to analysis by HPLC.

### 2.3. *Analytical methods*

The amounts of LG and GLC in the reaction mixtures were quantified by HPLC. The HPLC instrument was equipped with Agilent 1200 pump, a Bio-Rad organic acid column (Aminex HPX-87 H)-operated at 60 °C, a Waters 410 differential refractive index detector and a UV detector. The mobile phase consisted of aqueous sulfuric acid (5 mM) at a flow rate of 0.55 ml $min^{-1}$. The Injection volume of the sample was set at 5 μL. Calibration curves of standard solutions with known concentrations were used to determine the concentration of compounds in the product mixture. A typical HPLC chromatogram of a sample is shown in the Supplementary information (Figure S2).

### 2.4. *Definitions*

The concentrations of the relevant compounds involved in the reaction were determined by HPLC. These concentrations were used to calculate the conversion of LG ($X_{LG}$) and the yield of GLC ($Y_{GLC}$) according to the definitions given in Eqs. (1) and (2).

$$X_{LG} = \frac{(C_{LG,0} - C_{LG})}{C_{LG,0}}.100\% \quad (1)$$

$$Y_{GLC} = \frac{C_{GLC}}{C_{LG,0}}.100\% \quad (2)$$

## 3. Results and discussion

### 3.1. *Batch experiments: Product distribution, mass balances and reproducibility*

The conversion of LG with Amberlyst 16 as the solid acidic catalyst in water was performed in a batch set-up in a broad range of reaction conditions (352–388 K, $C_{LG,0}$ = 100–1000 mol $m^{-3}$ and a catalyst loading between 1 and 5 wt% on LG) at various stirring speeds. An example of a concentration versus time profile for LG and GLC ($C_{LG,0}$ = 1000 mol $m^{-3}$, 5 wt% catalyst, 500 rpm at 388 K) is shown in Fig. 1 (left). At these conditions, LG is nearly fully converted to GLC within 60 min. At prolonged reaction times, the concentration of GLC is slightly reduced. This is most likely due to subsequent reactions of GLC to for instance HMF, levulinic acid (LA), formic acid (FA) and humins (insoluble polymers) (Girisuta et al., 2006). The formation of LA, FA (HPLC) and/or humins (by visual observations) was not observed for all experiments. HMF was detected in a very small amount when T > 370 K. However, the amounts were too limited to allow accurate quantification.

Furthermore, mass (carbon) balance calculations were conducted based on the total amount of HPLC detectables (LG and GLC, excluding HMF, as it is only detected as traces) and the LG intake. The results are given in Fig. 1 (right) and show that carbon balance closure is quantitative from the beginning of the reaction until about 90 min. Above 90 min, a slight decrease in the carbon balance closure is apparent. This is due to limited decomposition of GLC, also visible in the GLC concentration versus time profile at extended batch times (Fig. 1, left). The level of decomposition of GLC is by far lower than found in our previous study using sulfuric acid (Abdilla et al., 2018), implying that Amberlyst 16 is more preferred than sulfuric acid when aiming for high GLC yields.

The reproducibility of the experiments was tested by performing a number of duplicate experiments. The results are given in Figure S3 (Supplementary information) and indicate that reproducibility of the experiments is good.

### 3.2. *Assessment of mass transfer limitations in batch experiments*

The conversion of LG to GLC in water using a solid Amberlyst 16 catalyst is an example of a heterogeneous reaction system. As such, diffusion limitations of LG, both externally and inside the porous Amberlyst particles, may occur and affect the conversion and yield of the process. To test the possibility of external mass-transfer limitations of LG from the liquid bulk to the catalyst surface, the effect of stirring rate on the LG conversion was determined and the results are presented in Fig. 2. It is evident that within the tested range of stirring speeds (250–1000 rpm), the conversion of LG does not depend on the stirring rate. From this observation, we conclude that external mass-transfer limitation of LG is absent.

To investigate whether intra-particle mass transfer limitations are of importance, the Weisz-Prater criterion (Vannice and Joyce, 2005) ($N_{W\text{-}P}$) was determined for a number of representative experiments (Table 1, see Supplementary information for calculation details). According to this criterion, a value of ≤0.3 implies the absence of intra-particle mass transfer limitations.

The Weisz–Prater criterion was found in the range between 0.25 and 2.77, indicating that most experiments were per-

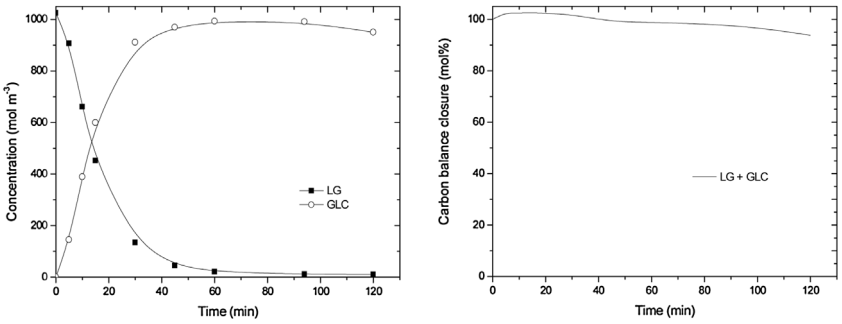


**Fig. 1 – Representative example of a concentration-time profile in batch (left) and carbon balance closure (right) at 388 K, $C_{LG,0}$ = 1000 mol m$^{-3}$ and 5 wt% catalyst at 500 rpm.**

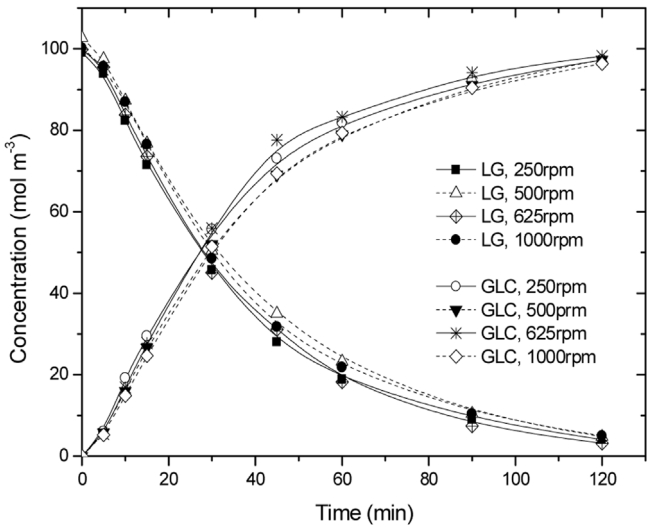


**Fig. 2 – Effect of stirring rate on LG conversion to GLC with Amberlyst 16 ($C_{LG,0}$ = 100 mol m$^{-3}$, 388 K and 2 wt% catalyst).**

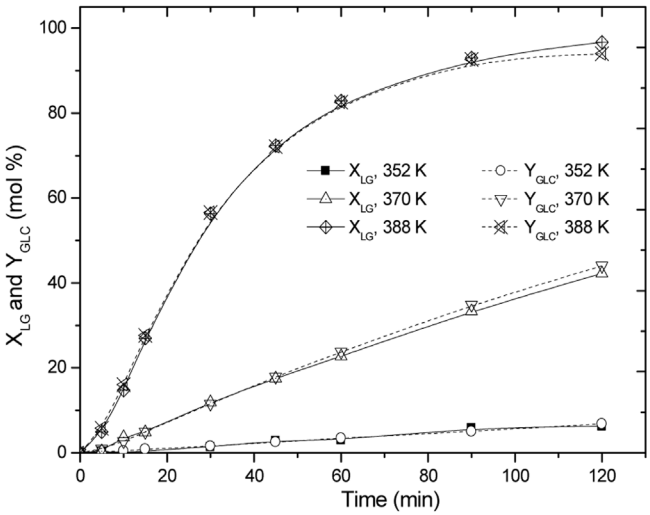


**Fig. 3 – Conversion of LG and yield of GLC versus time at different temperatures ($C_{LG,0}$ = 1 M, $W_{cat}$ = 2 wt%, at stirring speed of 500 rpm).**

**Table 1 – Calculated values for the Weisz-Prater criterion ($N_{W-P}$) for a number of representative experiments.**

| T, K | $W_{cat}$[a], g | $C_{LG,0}$, mol m$^{-3}$ | $N_{W-P}$ |
|---|---|---|---|
| 388 | 0.1 | 100 | 1.64 |
| 352 | 0.05 | 100 | 0.26 |
| 370 | 0.05 | 100 | 0.78 |
| 388 | 0.05 | 100 | 2.59 |
| 370 | 0.05 | 500 | 0.98 |
| 388 | 0.05 | 500 | 2.77 |
| 352 | 0.1 | 100 | 0.16 |
| 370 | 0.1 | 100 | 0.79 |
| 370 | 0.1 | 500 | 0.83 |
| 388 | 0.1 | 500 | 1.75 |
| 370 | 0.25 | 100 | 0.63 |
| 388 | 0.1 | 1000 | 1.69 |
| 388 | 0.25 | 1000 | 0.48 |

[a] Catalyst intakes of respectively 0.05, 0.1 and 0.25 g correspond to catalyst loadings of 1, 2 and 5 wt%.

formed in a regime where the overall rate is affected by intra-particle diffusion limitation of LG. As such, this effect was considered in the kinetic modeling studies (vide infra).

### 3.3. *Effect of process conditions on the conversion of LG to GLC in batch*

The effects of various process conditions on the conversion of LG and the GLC yield were determined experimentally. The temperature has a major effect on the rate of the reaction, see Fig. 3 for details. For instance, at a temperature of 388 K, 96 mol% of LG conversion ($X_{LG}$) was obtained after 2 h and it dropped to 45 mol% at lower temperature (370 K). The LG conversion versus time curve follows the trend of the GLC yield versus time curve, indicating that the reaction is very selective with GLC as the sole product.

The effect of the catalyst loading (wt% on LG) on the LG conversion vs time (370 K and $C_{LG,0}$ = 100 mol m$^{-3}$, 500 rpm) is given in Supplementary information (see Figure S4, left side). A linear relation between the initial reaction rate and the catalyst loading was observed (see Figure S4, right side), indicating a first order dependency in catalyst.

The effect of the initial concentrations of LG on the conversion of LG was determined ($C_{LG,0}$ = 100 – 1000 mol m$^{-3}$, 388 K and 5 wt% catalyst) and the results are given in Fig. 4 (left). The conversion of LG is essentially independent on the initial concentration of LG, indicating that the reaction order in LG is close to one. The rate of the undesired decomposition reaction of GLC, however, seems a function of the LG concentration, with high concentrations leading to a lower GLC yield (see Fig. 4 (right)). This implies that the rate of the decomposition reaction is concentration dependent and has an order higher than 1. The maximum yield of GLC was close to quantitative (98.5 mol%) when the reaction was carried out with 5 wt% of Amberlyst 16, an initial LG concentration of 500 mol m$^{-3}$, 388 K, 500 rpm and at batch time of 60 min.

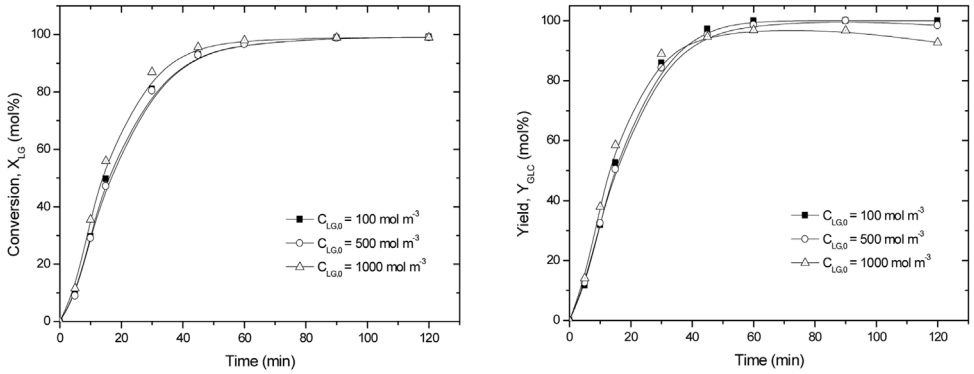


**Fig. 4 – Effect of initial LG concentration on LG conversion, $X_{LG}$ (left) and yield of GLC, $Y_{GLC}$ (right) at reaction conditions: 388 K, 5 wt% catalyst and stirring speed of 500 rpm.**

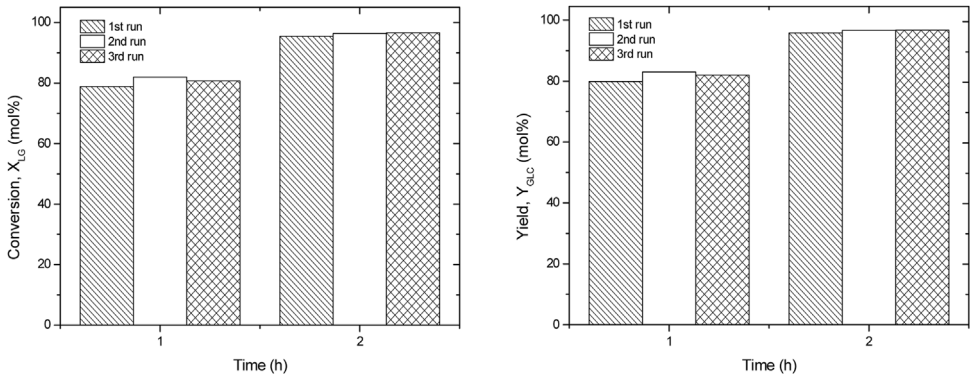


**Fig. 5 – Determination of catalyst stability by successive batch experiments showing $X_{LG}$ (left) and yield of GLC, $Y_{GLC}$ (right) vs the number of runs at 388 K, $C_{LG,0}$ = 100 mol m$^{-3}$, 2 wt% catalyst and a stirring speed of 500 rpm.**

### 3.4. *Catalyst stability*

Catalyst stability was tested in the batch set-up by performing three successive experimental runs (388 K, $C_{LG,0}$ = 100 mol m$^{-3}$, 2 wt% catalyst and a stirring speed of 500 rpm). After each run, the Amberlyst 16 catalyst was collected, washed with Milli-Q water and dried at 323 K for 4 h before a next run. The results are compiled in Fig. 5. Clearly, the LG conversion and GLC yield are not affected after 3 runs, indicating that catalyst stability is good.

### 3.5. *Kinetic model development*

A kinetic model for the reaction of LG in water with Amberlyst 16 as the catalyst was developed based on a simplified mechanism where LG is converted to GLC as a sole product (Scheme 1), justified by the very good carbon balance closures and excellent selectivity of the reaction. The LG and GLC component balances for the batch rector with the assumption of a constant liquid volume are given in Eqs. (3) and (4).

$$V_{liquid}\frac{dC_{LG}}{dt} = -R'_{LG}W_{cat} \tag{3}$$

$$V_{liquid}\frac{dC_{GLC}}{dt} = R'_{LG}W_{cat} \tag{4}$$

where $R'_{LG}$ denotes the LG reaction rate based on the weight of catalyst. The reaction is taken as a first order in LG, as confirmed by experiments with different initial LG concentrations (Fig. 4) and proceeds in the catalyst particles. The LG concentration in the catalyst particles can differ from the aqueous phase concentrations if the rate of diffusion of LG cannot keep up with the reaction rate. In that case the actual reaction rate is lower than the reaction rate based on bulk concentrations. Indeed, assessment of the WP criterion for the system reveals that intra-particle diffusion limitation of LG play a role (*vide supra*). To incorporate this effects the reaction rate is expressed as:

$$R'_{LG} = k'C_{LG}\eta_{cat} \tag{5}$$

where $\eta_{cat}$ denotes the catalyst effectiveness factor ($\eta_{cat} \leq 1$).

The reaction rate constant varies with the temperature according to an Arrhenius equation (Eq. 6) that depends on two parameters, the reaction rate constant at the reference temperature of 373 K, $k'_{373}$, and the activation energy, $E_a$:

$$k' = k'_{373}\exp\left[\frac{-E_a}{R}\left(\frac{1}{T}-\frac{1}{373}\right)\right] \tag{6}$$

The temperature in the batch reactor increases over time from the initial, $T_i$ to the set point value of the heating bath, $T_{setpoint}$ as given by Eq. (7) (for details see the Supplementary information).

$$T_{bulk} = T_{setpoint} - \left(T_{setpoint} - T_{bulk,i}\right)e^{-ht} \tag{7}$$

The reactor temperatures calculated from Eq. (7) are shown in the Supplementary information (Figure S5). It shows that the set-point is reached within a couple of minutes. As such, for reaction performed at particularly the highest temperature where the reaction rates are highest, the non-isothermal trajectory may have to be considered in the kinetic modeling (vide infra). The temperature of the catalyst particles is expected to closely follow the liquid bulk temperature and any difference

**Table 2 – Experimental conditions employed for the kinetic measurements.**

| Parameter | Values |
|---|---|
| $C_{LG,0}$ (mol/m$^3$) | 100, 500, 1000 |
| Catalyst loading (wt%) | 1, 2, 5 |
| $T_{setpoint}$ (K) | 352, 370, 388 |

between the two and any temperature gradients inside the catalyst particles are assumed negligible. For first order reactions the effectiveness factor of the catalyst is given by the well-known equation (Fogler, 1999).

$$\eta_{cat} = \frac{3}{\phi}\left(\frac{1}{\tanh\phi} - \frac{1}{\phi}\right) \quad (8)$$

where the Thiele modulus, $\phi$, is defined as:

$$\phi = R\sqrt{\frac{k'\rho_{cat}}{D_{eff}}} \quad (9)$$

### 3.6. Modeling approach

Experimental data were obtained at the conditions given in Table 2. For each of the possible 27 combinations of reaction conditions a sequence of 8 batch experiments was performed with reaction times ranging from 5 to 120 min (300–7200 s). Concentration-time profiles of all the batch experiments are available in the Supplementary information (Figure S6).

The model, consisting of Eq, (3)–(9), was fitted to the experimental data using MATLAB software. The diffusion coefficient of LG was obtained from the Wilke–Chang equation (see Supplementary information). The effective diffusivity of LG in the catalyst particle was estimated as: $D_{eff} = (\varepsilon/\tau)D_{LG}$ with $(\varepsilon/\tau) = 0.1$. The objective function in the optimization of the reaction rate was the sum of squared relative residuals, SSR, according to:

$$SSR = \sum_i \left(\frac{C_{model} - C_{experimental}}{C_{experimental}}\right)_i^2 \quad (10)$$

where the summation is over all of the experimental data. Using relative residuals here ensures that more or less equal weights are attributed to the data points despite the variation in the magnitude of the concentrations. The 95% parameter confidence intervals were obtained by adjusting the parameters until the SSR increases to a value given by Eq. (11):

$$SSR_{0.95} = SSR_{min}\left[1 + \frac{m}{N-m}F(m, N-m, 0.95)\right] \quad (11)$$

where F (m,N–m,0.95) is the value of the Fisher distribution at a 95% confidence level with (m,N – m) degrees of freedom (Draper and Smith, 2014).

### 3.7. Modelling results

The values of the parameters $k'_{373}$ and $E_a$ in Eq. (6) were fitted to all experimental data simultaneously. The resulting equation for the reaction rate is given as:

$$k' = (6.08 \pm 0.51) \times 10^{-6} \exp\left[\frac{-(132.3 \pm 10.1) \times 10^3}{R}\left(\frac{1}{T} - \frac{1}{373}\right)\right] \quad (12)$$

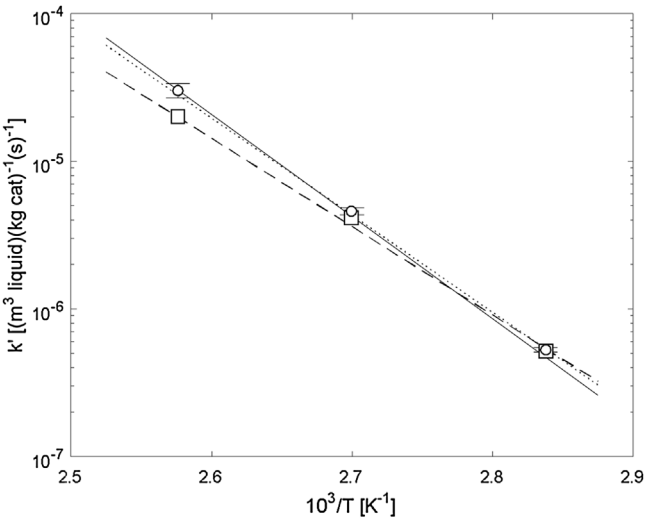


**Fig. 6 – Arrhenius plot of the conversion rate constant of LG to GLC. Solid line: fitted through all the data, see Eq. (12). Circles and horizontal bars: average and standard deviation of 9 sequences consisting of 8 batch experiments each. Dotted line: isothermal conditions assumed. Dashed line and squares: diffusion limitations assumed absent.**

The activation energy for the reaction is $132.3 \pm 10.1$ kJ mol$^{-1}$ and this value is somewhat higher compared to the ones found in the literature for soluble mineral acids. For instance, the activation energy for the conversion of LG to GLC using sulfuric acid as the catalyst in the temperature range of 323–403 K was reported to be 114 kJ mol$^{-1}$ (Helle et al., 2007), whereas we recently obtained a value of 123.4 kJ mol$^{-1}$ for a temperature range between of 353–433 K (Abdilla et al., 2018).

The reaction rate according to Eq. (12) is plotted in Fig. 6 (solid line). The influence of the non-isothermal conditions (Figure S7, Supplementary information) on the final outcome is small as shown by small deviation of the dotted line in Fig. 6. The latter was obtained by assuming that the reactor temperature was always equal to the setpoint temperature. This approach was inspired by Figure S7 where the reactor temperatures are shown to deviate from the setpoint temperatures only for the first 2 to 3 min, compared to a total reaction time of 2 h. Also shown in Fig. 6 are the results obtained by neglecting any diffusion limitation in the catalyst particles. The observed values of the rate constants, equal to $\eta_{cat}k'$, are shown as squares and the dashed line. Specifically at the highest temperature applied here the difference between the observed and intrinsic values of the reaction rate is substantial: $1.55 \times 10^{-5}$ vs $3.16 \times 10^{-5}$ m$^3$ kg$^{-1}$ s$^{-1}$ respectively.

The effectiveness factors from Eq. (8) show that the experiments at the highest temperature applied suffered from significant diffusion limitation, with an effectiveness factor as low as 0.68. The variation of the catalyst effectiveness factor as a function of the temperature is illustrated in Figure S8, (Supplementary information).

The assumption of a first order dependency of the reaction rate on the LG concentration is very plausible because of the excellent fit of the Arrhenius plot, see Fig. 6. The first order kinetics are further substantiated by considering the plot of the relative concentrations vs the time multiplied with the amount of catalyst in the reactor. Fig. 7 and 8 show these plots for all the experimental results obtained at 388 K. The data plotted in Fig. 7 and 8 converge on a single curve. This type of

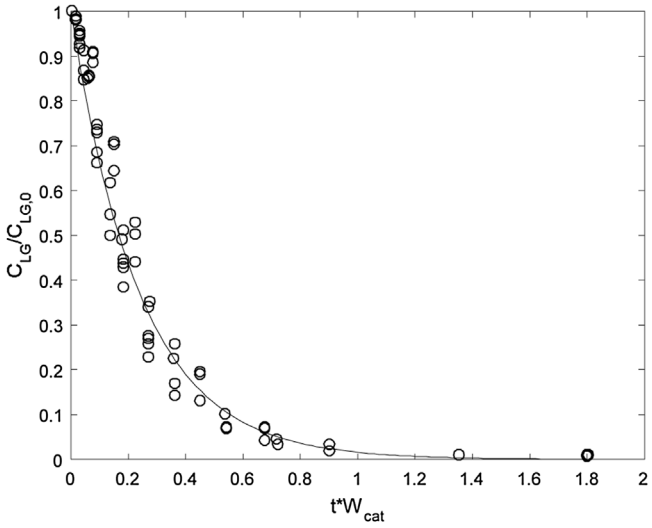


**Fig. 7 – Relative LG concentrations vs t x $W_{cat}$ at 388 K. Symbols: experimental data obtained with 9 sequences where $C_{LG,0}$ = 100, 500 and 1000 mol $m^{-3}$, and the catalyst loading is 1, 2 and 5 wt%. Line: model calculations using the result of Eq. (12).**

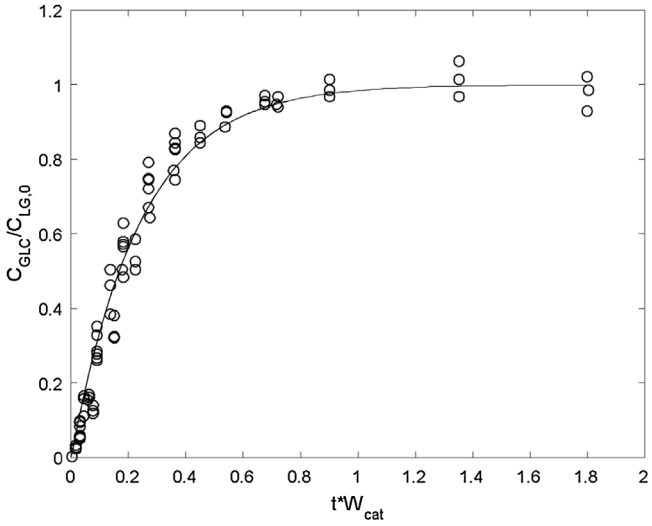


**Fig. 8 – Relative GLC concentrations vs t x $W_{cat}$ at 388 K. Symbols and line: see Fig. 7.**

behavior is obtained only with a first order reaction. With other reaction orders the results plotted according to this method cannot be represented by a single line.

### 3.8. *Model implications*

With the kinetic models available, it is possible to gain insight into LG conversion, selectivity and yield of GLC as a function of the process conditions. For instance, a simulation of the typical batch time needed to achieve 90 mol% LG conversion with 0.1 g Amberlyst 16 as catalysts at various temperatures is given in Fig. 9.

## 4. Continuous experiments in a packed bed reactor

The Amberlyst catalyst was tested for its performance in the hydrolysis of LG over extended time periods in a packed bed reactor (Figure S1, Supplementary information). In total, three runs with of up to 30 h run time were performed with a feed

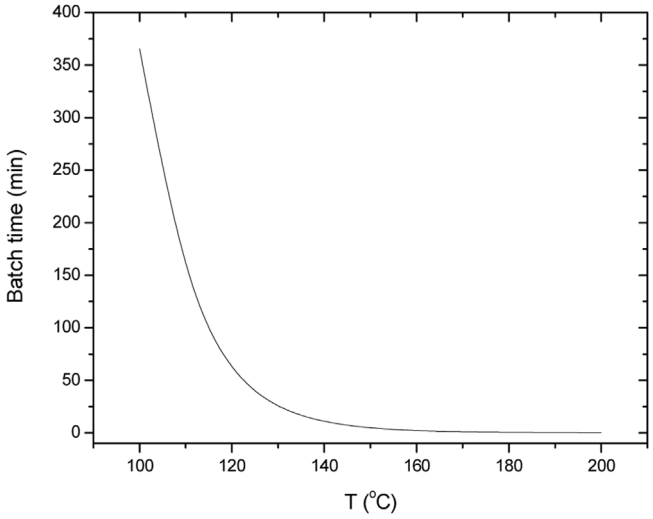


**Fig. 9 – Required batch time for $X_{LG}$ = 90 mol% as a function of T ($C_{LG,0}$ = 0.1 M, $W_{cat}$ =0.1 g).**

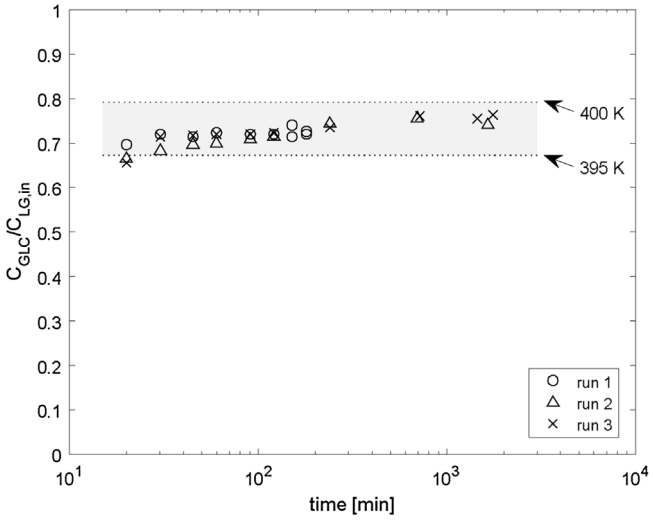


**Fig. 10 – Glucose yields versus runtime for triplicate packed bed experiments. Symbols: measured data points. Grey area: calculated from Eq (15) over the temperature range of.395–400 K.**

consisting of 0.1 M of LG with a flow rate of 2.2 ml $min^{-1}$ (WHSV = 1.65 $min^{-1}$). The results of the three runs are given in Fig. 10. The system reaches a steady state within 30 min, where the conversion of LG reached 73 mol% on average. Higher LG conversions were not aimed, as very high conversions hamper determination of catalyst stability. Selectivity is close to quantitative and other byproducts were not identified (HPLC). Moreover, it is also apparent from the three (triplicate) runs that the reproducibility of the system is good. In addition, catalyst stability also seems on par, at least for 30 h runtimes, in line with the batch recycle experiments.

The packed bed reactor was modeled as an ideal plug flow reactor. The component balance for a plug flow reactor reads:

$$v_s \frac{dC_{LG}}{dx} = -k' \eta_{cat} C_{LG} \frac{W_{cat}}{V_R} \quad (13)$$

In Eq. (13) any effects due to diffusion limitation in the catalyst is taken into account via the catalyst effectiveness factor

$\eta_{cat}$. Any external (gas-to-liquid) mass transfer limitations are assumed negligible here. Integration of Eq. (13) gives:

$$\frac{C_{LG}}{C_{LG,0}} = \exp\left[-\frac{\eta_{cat} W_{cat} k'}{\phi_v}\right] \quad (14)$$

and:

$$\frac{C_{GLC}}{C_{LG,0}} = 1 - \frac{C_{LG}}{C_{LG,0}} = 1 - \exp\left[-\frac{\eta_{cat} W_{cat} k'}{\phi_v}\right] \quad (15)$$

Experimentally some difficulties in controlling the temperature were encountered, resulting in some variation of the operating temperature of the reactor around the set point. The inlet reactor temperature was found to be 398 K, the exit temperature was 388 K. This difference is likely due to heat losses to the environment due to insufficient isolation. Therefore, in Fig. 10, we compare the experimental results of the packed bed reactor with modeling results over the temperature range of 395–400 K. It can be concluded that the kinetic model derived in batch including intra-particle mass transfer limitations describes the experimental runs in the packed bed reactor well and confirms its validity.

## 5. Conclusions

An experimental study on the conversion of LG to GLC with a solid Amberlyst 16 catalyst in water was performed in a batch set-up using a wide range of process conditions (250–1000 rpm, initial LG concentration between 100–1000 mol $m^{-3}$, 352–388 K and a catalyst loading between 1–5 wt%) The highest GLC yield was 98.5 mol% (388 K, 5 wt% Amberlyst 16, $C_{LG,0}$ = 500 mol $m^{-3}$ at 500 rpm stirring rate and t=60 min).The data were successfully modeled assuming a first order reaction in LG and incorporation of intra-particle diffusion limitation of LG. The activation energy was found to be 132.3 ± 10.1 kJ $mol^{-1}$. Catalyst stability was assessed by recycle runs in batch and continuous experiments in a packed bed reactor. Catalyst activity was stable for runtimes up to 30 h, indicating good catalyst stability, supported by the batch recycle experiments. The steady state conversion levels in the packed bed reactor were successfully modelled using the kinetic model from the batch data.

## Acknowledgement

R.M. Abdilla-Santes express gratitude to the Directorate General of Higher Education, Ministry of Education and Culture, Indonesia for funding of her PhD program. C.B. Rasrendra acknowledges ITB for receiving a WCU-ITB grant. The authors also thank Jan Henk Marsman, Leon Rohrbach, Erwin Wilbers, Marcel de Vries, and Anne Appeldoorn for analytical and technical support, and Henk van de Bovenkamp for input in the reactor modelling.

## References

Corma, A., Iborra, S., Velty, A., 2007. Chemical routes for the transformation of biomass into chemicals. Chem. Rev. 107, 2411–2502.

Ragauskas, A.J., Williams, C.K., Davison, B.H., Britovsek, G., Cairney, J., Eckert, C.A., Frederick Jr., W.J., Hallett, J.P., Leak, D.J., Liotta, C.L., Mielenz, J.R., Murphy, R., Templer, R., Tschaplinski, T., 2006. The path forward for biofuels and biomaterials. Science (New York, N.Y.) 311, 484–489.

van Putten, R., van der Waal, Jan C., De Jong, E., Rasrendra, C.B., Heeres, H.J., de Vries, J.G., 2013. Hydroxymethylfurfural, a versatile platform chemical made from renewable resources. Chem. Rev. 113, 1499–1597.

http://www.btgworld.com/en/rtd/technologies/fast-pyrolysis, 7 December 2016.

Lian, J., Chen, S., Zhou, S., Wang, Z., O'Fallon, J., Li, C., Garcia-Perez, M., 2010. Separation, hydrolysis and fermentation of pyrolytic sugars to produce ethanol and lipids. Bioresour. Technol. 101, 9688–9699.

Bennett, N.M., Helle, S.S., Duff, S.J., 2009. Extraction and hydrolysis of levoglucosan from pyrolysis oil. Bioresour. Technol. 100, 6059–6063.

Bykova, M., Ermakov, D.Y., Kaichev, V., Bulavchenko, O., Saraev, A., Lebedev, M.Y., Yakovlev, V., 2012. Ni-based sol–gel catalysts as promising systems for crude bio-oil upgrading: guaiacol hydrodeoxygenation study. Appl. Catal. B 113, 296–307.

Oasmaa, A., Kuoppala, E., Ardiyanti, A., Venderbosch, R., Heeres, H., 2010. Characterization of hydrotreated fast pyrolysis liquids. Energy Fuels 24, 5264–5272.

Wang, H., Male, J., Wang, Y., 2013. Recent advances in hydrotreating of pyrolysis bio-oil and its oxygen-containing model compounds. ACS Catal. 3, 1047–1070.

Zacher, A.H., Olarte, M.V., Santosa, D.M., Elliott, D.C., Jones, S.B., 2014. A review and perspective of recent bio-oil hydrotreating research. Green Chem. 16, 491–515.

Ardiyanti, A., Khromova, S., Venderbosch, R., Yakovlev, V., Heeres, H., 2012. Catalytic hydrotreatment of fast-pyrolysis oil using non-sulfided bimetallic Ni-Cu catalysts on a δ-Al 2 O 3 support. Appl. Catal. B 117, 105–117.

Elliott, D.C., Hart, T.R., Neuenschwander, G.G., Rotness, L.J., Zacher, A.H., 2009. Catalytic hydroprocessing of biomass fast pyrolysis bio-oil to produce hydrocarbon products. Environ. Prog. Sustain. Energy 28, 441–449.

Scholze, B., Meier, D., 2001. Characterization of the water-insoluble fraction from pyrolysis oil (pyrolytic lignin). Part I. PY–GC/MS, FTIR, and functional groups. J. Anal. Appl. Pyrolysis 60, 41–54.

Venderbosch, R., Ardiyanti, A., Wildschut, J., Oasmaa, A., Heeres, H., 2010. Stabilization of biomass-derived pyrolysis oils. J. Chem. Technol. Biotechnol. 85, 674–686.

Rover, M.R., Johnston, P.A., Jin, T., Smith, R.G., Brown, R.C., Jarboe, L., 2014. Production of clean pyrolytic sugars for fermentation. ChemSusChem 7, 1662–1668.

Abou-Yousef, H., Steele, P., 2013. Increasing the efficiency of fast pyrolysis process through sugar yield maximization and separation from aqueous fraction bio-oil. Fuel Process. Technol. 110, 65–72.

Wang, Yin, 2017. Catalytic Hydrotreatment of Pyrolysis Liquids and Fractions: Catalyst Development and Process Studies (Doctoral Dissertation). Groningen.

Helle, S., Bennett, N.M., Lau, K., Matsui, J.H., Duff, S.J., 2007. A kinetic model for production of glucose by hydrolysis of levoglucosan and cellobiosan from pyrolysis oil. Carbohydr. Res. 342, 2365–2370.

Bozell, J.J., Petersen, G.R., 2010. Technology development for the production of biobased products from biorefinery carbohydrates — the US Department of Energy's "top 10" revisited. Green Chem. 12, 539–554.

Vidrio, E., 2004. Study of the kinetics of the acid-catalyzed hydrolysis of levoglucosan. McNair Scholars J 5, 90–103.

Abdilla, R., Rasrendra, C., Heeres, H., 2018. Kinetic studies on the conversion of Levoglucosan to glucose in water using brønsted acids as the catalysts. Ind. Eng. Chem. Res. 57, 3204–3214.

Girisuta, B., Janssen, L.P.B.M., Heeres, H.J., 2006. Green chemicals: a kinetic study on the conversion of glucose to levulinic acid. Chem. Eng. Res. Des. 84, 339–349.

Vannice, M.A., Joyce, W.H., 2005. Kinetics of Catalytic Reactions. Springer.

Fogler, H., 1999. Elements of Chemical Reaction Engineering, 3rd ed. Prentice Hall.

Draper, N.R., Smith, H., 2014. Applied Regression Analysis. John Wiley & Sons.